



ELSEVIER

1 April 2002

Optics Communications 204 (2002) 247–251

OPTICS
COMMUNICATIONS

www.elsevier.com/locate/optcom

Site dependent thermoluminescence of long persistent phosphorescence of $\text{BaAl}_2\text{O}_4:\text{Ce}^{3+}$

D. Jia^a, Xiao-jun Wang^{b,*}, E. van der Kolk^a, W.M. Yen^a^a Department of Physics and Astronomy, University of Georgia, Athens, GA 30602, USA^b Department of Physics, Georgia Southern University, Statesboro, GA 30460-8031, USA

Received 27 February 2002; accepted 27 February 2002

Abstract

A very long persistent phosphor $\text{BaAl}_2\text{O}_4 : \text{Ce}^{3+}$ was prepared and studied. The Ce^{3+} 5d-4f emissions from two Ba^{2+} sites in the BaAl_2O_4 were observed at 450 and 402 nm. The lowest 4f-5d excitation peaks were recorded at 357 and 335 nm, respectively. The persistence times of the long afterglow emissions from Ce^{3+} at the two sites were found to be longer than 10 h. Site-selective thermoluminescence spectra of the sample were measured. Two sets of thermoluminescence peaks were detected at -43 , -26 and 27 °C, and -53 , -36 and 30 °C (heating rate 13.3 °C/min) corresponding to the two sites at 450 nm (site-1) and 402 nm (site-2), respectively. Dy^{3+} , Ce^{3+} co-doped samples were also prepared, which introduce new defect-related traps at 18, 50, and 82 °C (heating rate 10 °C/min). These defect-related traps due to Dy^{3+} co-doping also contribute to the Ce^{3+} afterglow at the two sites. © 2002 Elsevier Science B.V. All rights reserved.

PACS: 78.60; 78.55; 61.72; 42.30

Keywords: Thermoluminescence; Electron trap; Electron migration; Afterglow

1. Introduction

Long persistence materials have potential in many commercial applications in signing and display. In recent years, the study of long persistence materials was switched to rare earth ion doped alkali earth aluminates [1,2] from alkali earth sulfides, because the persistence time of rare earth ion

doped aluminates is about 10 times longer than that of doped sulfides [3,4]. The aluminate hosts usually have more complicated structures than sulfide hosts, which may generate more defect-related traps when they are doped with rare earth ions.

The alkali earth aluminate of interest in this paper is BaAl_2O_4 . It has a very high melting point (1815 °C) and holds a stuffed tridemite (hexagonal) structure with lattice parameter of $a = 10.449$ Å and $c = 8.793$ Å. The BaAl_2O_4 belongs to $C_6^6\text{-P}6_3$ space group. There are two different Ba^{2+} sites, one site (site-1) is twice as abundant as the other (site-2) [5–7]. Ba^{2+} has an ionic radius $r = 1.34$ Å that is

* Corresponding author. Tel.: +1-912-681-5503; fax: +1-912-681-0471.

E-mail address: xwang@gasou.edu (X.-j. Wang).

much bigger than most of the trivalent rare earth ions so that the rare earth dopants can easily substitute for the Ba^{2+} sites. BaAl_2O_4 has been studied as a host for Eu^{2+} because the $\text{BaAl}_2\text{O}_4 : \text{Eu}^{2+}, \text{Dy}^{3+}$ system shows a long afterglow [8,9]. In contrast with Eu^{2+} , to our knowledge, the properties of Ce^{3+} have not been studied yet in BaAl_2O_4 host. The 4f-5d transitions of Ce^{3+} are allowed and are sensitive to changes in the crystal field [10,11]. Usually when a trivalent ion sits in a divalent ion site some defects will be created, producing defect-related traps that then result in a long afterglow [12]. This is also true for Ce^{3+} . When Ce^{3+} ions substitute for divalent ions, defect-related traps are generated and long afterglow appeared [13].

In this work, the long afterglow of Ce^{3+} emission in BaAl_2O_4 was observed by eye in darkness for as long as 10 h. Emission and excitation spectra from Ce^{3+} at the two different sites were measured. Site-selective thermoluminescence experiments were also performed. The experimental results showed that Ce^{3+} creates different defect-related traps at the different sites of Ba^{2+} . With the addition of Dy^{3+} , additional defect-related traps were observed.

2. Experimental

The $\text{BaAl}_2\text{O}_4 : \text{Ce}^{3+}$ (with/without Dy^{3+}) samples were prepared by sintering. 0.01 moles of each of BaCO_3 and Al_2O_3 were mixed. 0.5 at.% of $\text{Ce}_2(\text{CO}_3)_3$ (with/without 0.5 at.% of Dy_2O_3) and 5 at.% of B_2O_3 were added as activator and flux, respectively. The raw materials used in this work are all of 99.99% purity. The mixture was pressed into pellets and sintered at 900 °C for 2 h. The sintered pellets were then ground and pressed into pellets again to ensure better mixing. The pre-treated pellets were sintered at 1350 °C for 25 h in $\text{N}_2 + 5\% \text{H}_2$ gas flow.

Emission and excitation spectra and room temperature afterglow decay of the samples were recorded using a FluoroMaxII spectrometer or a Spex 500M spectrometer. The site-selective thermoluminescence spectra were measured by using a homemade vacuum cryostat, an Omega thermal controller, a Spex monochromator, and a

PMT. The light source to irradiate the samples was a mercury UV lamp.

3. Results and discussion

The emission and excitation spectra of Ce^{3+} at two different sites, site-1 and site-2, in BaAl_2O_4 are shown in Fig. 1. Fig. 1(a) shows that the emission peak of Ce^{3+} at Ba^{2+} site-1 at 450 nm (excited at 357 nm) and the lowest excitation peak at 357 nm (monitored at 450 nm) yield a Stokes shift of 5789 cm^{-1} . The emission (excited at 335 nm) and excitation (monitored at 402 nm) spectra of Ce^{3+} at Ba^{2+} site-2 are depicted in Fig. 1(b) with 4975 cm^{-1} Stokes shift. The differences in the emission and excitation spectra of the Ce^{3+} at

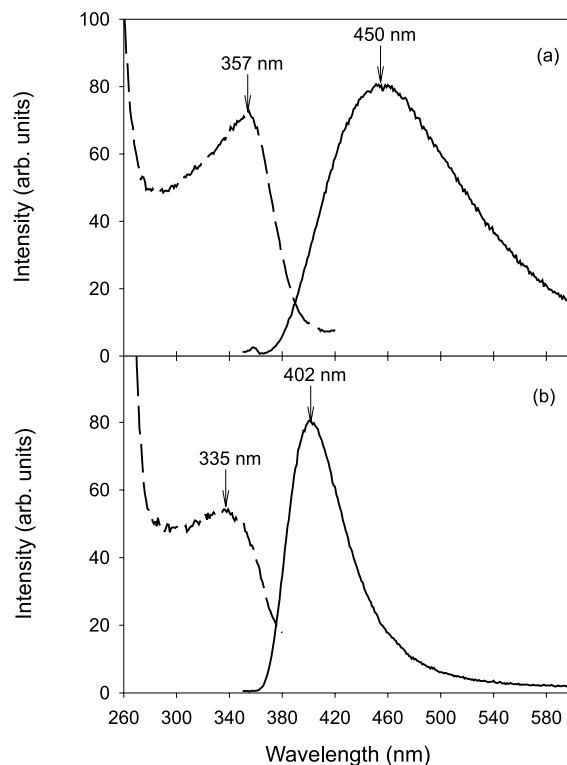


Fig. 1. Emission (solid lines) and excitation spectra (dashed lines) of Ce^{3+} doped BaAl_2O_4 phosphor. (a) Site-1, $\lambda_{\text{ex}} = 357 \text{ nm}$ for emission spectrum, $\lambda_{\text{em}} = 450 \text{ nm}$ for excitation spectrum. (b) Site-2, $\lambda_{\text{ex}} = 335 \text{ nm}$ for emission spectrum, $\lambda_{\text{em}} = 402 \text{ nm}$ for excitation spectrum.

different sites are due to the different environments of the two sites and the strong field dependence of the 4f-5d transition of the Ce^{3+} . The average Ba–O distance of site-1 and site-2 are 2.85 and 2.94 Å, respectively. The ligand field at site-1 is stronger than that at site-2 and therefore the splitting of the 5d level of Ce^{3+} is larger at site-1 than at site-2. Thus the emission and excitation energy of site-1 are lower than that of site-2 [6].

The $BaAl_2O_4 : Ce^{3+}$ sample shows very long lasting afterglow, with a persistence time up to 10 h observed by eye in darkness. The long persistent afterglow decay curves at 402 and 450 nm emissions are shown in Fig. 2. The samples were irradiated by a mercury lamp for 10 min, and the afterglow was detected at the maximum of the emission for each site. At the initial afterglow decay, the intensity from site-1 is about three times of that from the site-2. This is in good agreement with the 2:1 concentration ratio of the two different sites.

The long afterglow of Ce^{3+} in $BaAl_2O_4$ host is due to the traps that are generated by Ce^{3+} substituting for Ba^{2+} . In general, if some non-charge-compensated substitutions occur, defect-related traps will be formed. Similar results were observed in $CaS : Bi^{3+}$ when Bi^{3+} replaces Ca^{2+} [14] and in $CaS : Eu^{2+}, Cl^-$ when Cl^- replaces S^{2-} although Cl^- is not an emission center [15]. These defect-related trapping centers can be filled by either

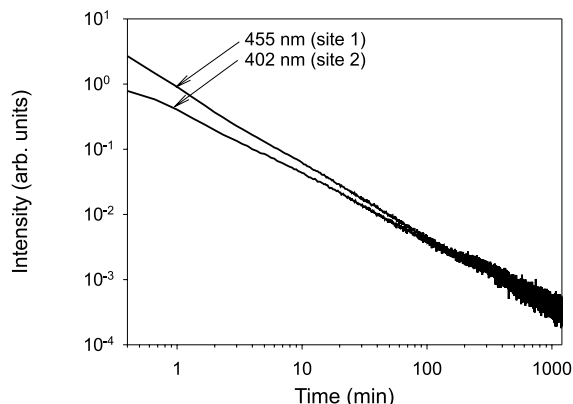


Fig. 2. Afterglow decays of $BaAl_2O_4 : Ce^{3+}$ from site-1 (450 nm) and site-2 (402 nm), respectively. (The sample was irradiated by a UV mercury lamp at room temperature for 10 min.)

electron transport through the conduction band, or tunneling through 5d states [13,16]. There are differences between these two types of trapping mechanisms. The tunneling process usually requires that the traps be close to the activator, so that electrons from the activator are able to tunnel into the nearby trap and vice versa. In the case of electron transport via the conduction band, the traps do not have to be located close to the activator, although the trapping rate may be distance dependent.

The nature of the Ce^{3+} induced electron traps is very interesting because there is site dependence of the defect-related electron traps. Thermoluminescence spectra were measured by detecting the thermally excited fluorescence of Ce^{3+} at the two emission wavelengths of 450 and 402 nm, respectively. The samples were cooled down to $-100\text{ }^\circ\text{C}$ and then irradiated by a mercury lamp for 30 min. Thermoluminescence spectra were then recorded by heating the sample at a rate of $13.3\text{ }^\circ\text{C}/\text{min}$ to $200\text{ }^\circ\text{C}$. The site-selective thermoluminescence spectra are shown in Fig. 3. The thermoluminescence peaks appear at $-53, -36$ and $30\text{ }^\circ\text{C}$ for the 402 nm emission at site-2 (Fig. 3(b)), and at $-43, -26$ and $27\text{ }^\circ\text{C}$ for site-1 at the 450 nm (Fig. 3(a)). The thermoluminescence spectra were also recorded by detecting the two emissions together. The result for the combination of the two sets of

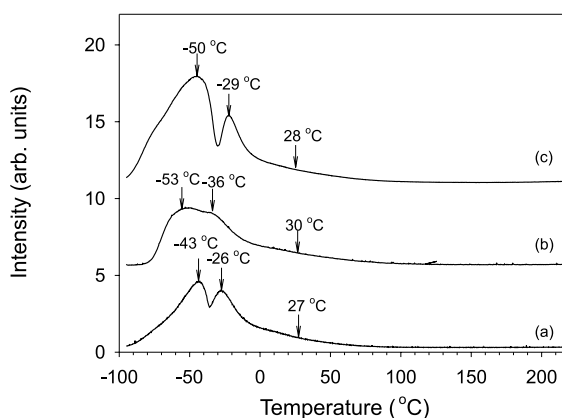


Fig. 3. Thermoluminescence spectra of $BaAl_2O_4 : Ce^{3+}$. Curves (a), (b), and (c) correspond to the emissions from site-1, site-2, and both sites, respectively. (The sample was irradiated by a UV mercury lamp for 30 min at $-100\text{ }^\circ\text{C}$ and heated to $200\text{ }^\circ\text{C}$ at a rate of $13.3\text{ }^\circ\text{C}/\text{min}$.)

thermoluminescence is shown in (Fig. 3(c)). The combination spectrum looks similar to that of 450 nm thermoluminescence, suggesting that the site-1 (emission at 450 nm) dominate the Ce^{3+} substitutions. These traps shown in Fig. 3 are the sources of the long afterglow of Ce^{3+} shown in Fig. 2.

The site dependence of the thermoluminescence spectra implies that the Ce^{3+} ions create different defect-related traps at different sites. These defect-related electron traps reside close to the corresponding Ce^{3+} emission centers. Although it is not certain if the electrons are trapped via tunneling or via transport through the conduction band, it is reasonable to assume that the electron excited from one site is trapped mostly by an electron trap near that site based on the site-dependent thermoluminescence results. The trapping process of the excited Ce^{3+} electrons is a short-range electron migration, and defect-related traps may also depend on the ligand environment of each site, and probably is the reason of different trap depths at different sites.

To investigate the electron migration in the trapping process, the thermoluminescence spectra of Ce^{3+} , Dy^{3+} co-doped sample were also measured. The co-doped sample is cooled down to $-100\text{ }^\circ\text{C}$ and then irradiated by the mercury lamp for 30 min. Thermoluminescence spectra were recorded by heating the sample at a rate of $10\text{ }^\circ\text{C}/\text{min}$ to $200\text{ }^\circ\text{C}$. The thermoluminescence spectra are shown in Fig. 4. Fig. 4(c) shows the thermoluminescence spectrum obtained by collecting all Ce^{3+} emissions from both sites. The thermoluminescence peaks at -68 , -49 , -26 and $-11\text{ }^\circ\text{C}$ most likely correspond to the defect-related electron traps created by Ce^{3+} . The additional thermoluminescence peaks at 18 , 50 and $82\text{ }^\circ\text{C}$ must be due to the traps created by co-doping with Dy^{3+} . The thermoluminescence spectra obtained by detecting the Ce^{3+} thermoluminescence at 450 and 410 nm shown in Figs. 4(a) and (b), respectively. The thermoluminescence signals are much weaker in comparison to the singly doped sample, because part of the luminescence of Ce^{3+} is quenched by Dy^{3+} . From Figs. 4(a) and (b), one can also find that the Dy^{3+} -created defect-related traps appear in the thermoluminescence at both sites. The Dy^{3+} ions and Ce^{3+} ions are doped uniformly so that the

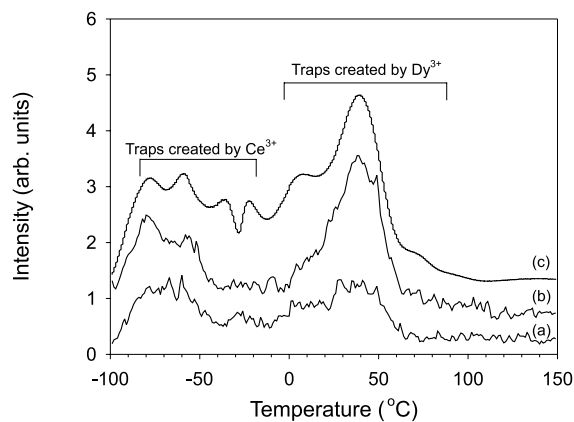


Fig. 4. Thermoluminescence spectra of $\text{BaAl}_2\text{O}_4 : \text{Ce}^{3+}, \text{Dy}^{3+}$. Curves (a), (b), and (c) correspond to the emissions from site-1, site-2, and both sites, respectively. (The sample is irradiated by UV mercury lamp for 30 min at $-100\text{ }^\circ\text{C}$ and heated to $200\text{ }^\circ\text{C}$ at a rate of $10.0\text{ }^\circ\text{C}/\text{min}$.)

average distance between Ce^{3+} and Dy^{3+} centers are about a couple of nanometer for 1 mol% concentration. If the Dy^{3+} creates traps similarly to Ce^{3+} , then the traps created by Dy^{3+} should also be close to Dy^{3+} . Therefore the appearance of the Dy^{3+} created defect-related electron traps indicates that electrons trapped by Dy^{3+} created traps should be due to the electron migration through conduction band. And thus the trapped electrons will migrate to both sites occupied by Ce^{3+} with almost equal probability. This electron transport through conduction band is possible because most of the 5d excited states of Ce^{3+} in aluminates host are close to (or even overlap with) the conduction band.

4. Conclusion

A long persistent phosphor $\text{BaAl}_2\text{O}_4 : \text{Ce}^{3+}$ was prepared and studied. The Ce^{3+} emissions were found at 402 and 450 nm due to the ions occupying two different sites of Ba^{2+} . The persistence times of the long afterglow of Ce^{3+} emissions at 402 and 450 nm were all longer than 10 h. The long afterglow was the result of Ce^{3+} created defect-related electron traps. Site selective thermoluminescence spectra implied that traps were close to the corre-

sponding Ce^{3+} ion. This short-range electron migration induces the site dependence of thermoluminescence. A Dy^{3+} co-doped sample was also studied. The electrons trapped by Dy^{3+} created defect-related electron traps may move to Ce^{3+} centers at both sites. This long-range process indicates that the electrons were transported through the conduction band.

Acknowledgements

This work was supported by the National Science Foundation under grant DMR 9986693. The authors wish to acknowledge the useful discussions with Dr. M. ter Heerdt. XJW is grateful for the support of Faculty Research Grant from Georgia Southern University.

References

- [1] S.H. Ju, U.S. Oh, J.C. Choi, H.L. Park, T.W. Kim, C.D. Kim, *Mater. Res. Bull.* 35 (2000) 1831.
- [2] T. Matsuzawa, Y. Aoki, N. Takeuchi, Y. Murayama, *J. Electrochem. Soc.* 143 (1996) 2670.
- [3] D. Jia, J. Zhu, B. Wu, *J. Electrochem. Soc.* 147 (2000) 386.
- [4] W. Jia, H. Yuan, L. Lu, H. Liu, W.M. Yen, *J. Lumin.* 76&77 (1998) 424.
- [5] S. Huang, R. von der Mühl, J. Ravez, J.P. Chaminade, P. Hagenmuller, M. Couzi, *J. Solid. Stat. Chem.* 109 (1994) 97.
- [6] T. Nakamura, K. Kaiya, N. Takahashi, T. Matsuzawa, C.C. Rowlands, V. Beltran-lopez, G.M. Smith, P.C. Riedi, *Phys. Chem. Chem. Phys.* 1 (1999) 4011.
- [7] S.H.M. Poort, W.P. Blokpoel, G. Blasse, *Chem. Mater.* 7 (1995) 1547.
- [8] J. Hölsä, H. Jungner, M. Lastusaari, J. Niittykoski, *J. Alloys Compd.* 323/324 (2001) 326.
- [9] R. Sakai, T. Katsumata, S. Komuro, T. Morikawa, *J. Lumin.* 85 (1999) 149.
- [10] P. Dorenbos, *Phys. Rev. B* 62 (2000) 15640, See also p. 15650; *J. Lumin.* 91 (2000) 155.
- [11] M. Bettinelli, R. Moncorge, *J. Lumin.* 92 (2001) 287.
- [12] D. Jia, J. Zhu, B. Wu, *J. Mater. Sci. Lett.* 20 (2001) 1313.
- [13] D. Jia, R.S. Meltzer, W.M. Yen, *J. Electrochem. Soc.*, submitted.
- [14] D. Jia, J. Zhu, B. Wu, *J. Lumin.* 91 (2000) 33.
- [15] D. Jia, J. Zhu, B. Wu, *J. Electrochem. Soc.* 147 (2000) 3948.
- [16] D. Jia, W. Jia, D.R. Evans, W.M. Dennis, H. Liu, J. Zhu, W.M. Yen, *J. App. Phys.* 88 (1999) 3402.